Quantum Coherence in the Time-Resolved Auger Measurement

Olga Smirnova, Vladislav S. Yakovlev, and Armin Scrinzi*

[1]*Photonics Institute, Vienna University of Technology, Gusshausstrasse 27/387, A-1040 Vienna, Austria/EU*

(Received 13 August 2003; published 15 December 2003)

We present a quantum mechanical model of the attosecond-XUV (extreme ultraviolet) pump and laser probe measurement of an Auger decay [Drescher *et al.*, Nature (London) **419**, 803 (2002)] and investigate effects of quantum coherence. The time-dependent Schrödinger equation is solved by numerical integration and in analytic form. We explain the transition from a quasiclassical energy shift of the spectrum to the formation of sidebands and the enhancement of high- and low-energy tails of the Auger spectrum due to quantum coherence between photoionization and Auger decay.

DOI: 10.1103/PhysRevLett.91.253001 PACS numbers: 32.80.Fb, 32.80.Hd

Recently developed XUV (extreme ultraviolet) light sources with subfemtosecond pulse durations [1,2] make it possible to directly observe and control the motion of valence electrons in atoms and molecules. In first experiments XUV pump—laser probe techniques were used to "steer" photoelectron packets by varying pump-probe delay and pulse intensity [3] and to obtain the time-resolved image of an Auger decay [4]. Although the basic physical ideas of the measurements can be phrased in terms of classical mechanics [5], the observed electron spectra are determined by quantum interference phenomena. In general, pumping, evolution of the excited electronic states, and probing must be treated as a single coherent quantum process. In this new type of time-resolved experiments time-independent approaches of traditional electron beam or synchrotron spectroscopy (see [6] for a review) are no longer applicable. Standard time-dependent methods employing wave-packet dynamics as for Rydberg atoms or in femtochemistry are inappropriate for the Auger process, where only few discrete levels are involved. Approaches developed for atoms in strong fields do not address the question of time-resolved observation [7,8]. As a result, for the interpretation of the time-resolved Auger measurement in Ref. [4] an *ad hoc* model was used, which combined a rate-equation description of core-hole formation and subsequent Auger decay with a quantum theory of laser probing [9,10]. That model becomes questionable in at least two cases: (i) at XUV-pulse durations similar to the Auger lifetime, when a two-stage description by first core-hole formation and then Auger decay is inadmissible and (ii) at decay times comparable to the laser period, when Auger electron spectra show features that are intermediate between the well-known formation of sidebands and quasiclassical "streaking" of electron energies [5].

In the present Letter we unite core-hole formation, Auger decay, and Auger electron streaking by the laser in a consistent quantum theory of time-resolved Auger measurement. The primary purpose of the work is to clarify the role of quantum coherence for the final Auger electron spectra. A set of basic equations is derived that is solved numerically as well as analytically. We find that in general the time-resolved measurement cannot be correctly described as a two-stage process of XUV ionization and subsequent independent Auger decay. Comparison to the two-stage *ad hoc* description of [4] shows that quantum coherence between photoelectrons and Auger electrons leads to a broadening of observed Auger spectra.

A scheme of the pump-probe Auger measurement is shown in Fig. 1. An XUV pulse with photon energy Ω excites a core electron with energy E_0 to a continuum energy near $W_x = E_0 + \Omega$. The vacancy is filled from the level E_a by Auger decay. The Auger electron is ejected from the level E_b to the final energy near $W_A = E_a + E_b - E_0$. A laser probe pulse modifies the Auger electron spectrum and spectra are recorded as a function of time delay Δt between XUV and laser pulse.

Our model is based on the essential states participating in the process: the ground state $|g\rangle$, the set of core-hole states $|h\rangle$ with one electron in the continuum, and the set of final states $|f\rangle$ with two continuum electrons. Disregarding for the present discussion correlation effects, the three states can be written as products of single-electron orbitals in the form

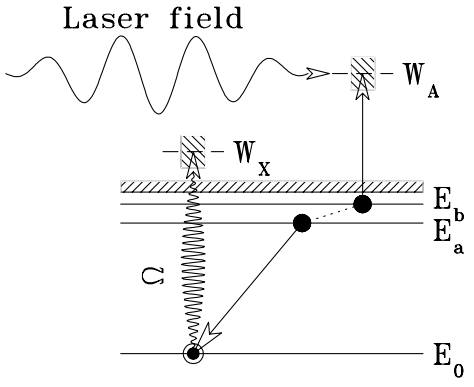

FIG. 1. Scheme of the Auger pump-probe measurement

$$|g, t\rangle = |0, t\rangle|a, t\rangle|b, t\rangle, \quad (1)$$

$$|h, t\rangle = |\mathbf{k}_x, t\rangle|a, t\rangle|b, t\rangle, \quad (2)$$

$$|f, t\rangle = |\mathbf{k}_x, t\rangle|0, t\rangle|\mathbf{k}_l, t\rangle. \quad (3)$$

The bound states $|0, t\rangle$, $|a, t\rangle$, and $|b, t\rangle$ with time dependence $\exp(-itE_\alpha)$, $\alpha = 0, a, b$ denote single-electron orbitals with the energies E_0, E_a, and E_b (cf. Fig. 1). The continuum states $|\mathbf{k}_x, t\rangle$ and $|\mathbf{k}_l, t\rangle$ are Volkov solutions for free electrons in the XUV and laser fields, respectively,

$$|\mathbf{k}_\eta, t\rangle = e^{-i\Phi_\eta(\mathbf{k}_\eta, t)} e^{i[\mathbf{k}_\eta - \mathbf{A}_\eta(t)]\cdot\mathbf{r}}, \qquad \eta = l, x, \quad (4)$$

where $\mathbf{A}_\eta$ and the Volkov phases Φ_η are given by

$$\mathbf{A}_\eta(t) = -\int_{-\infty}^{t} \mathcal{E}_\eta(t')dt', \quad (5)$$

$$\Phi(\mathbf{k}_\eta, t) = \frac{1}{2}\int_{-\infty}^{t} [\mathbf{k}_\eta - \mathbf{A}_\eta(t')]^2 dt', \quad (6)$$

and $\mathcal{E}_\eta$, $\eta = l, x$ denote the respective field strengths. Double occupation of the single-electron states is excluded by the construction of our essential states, if we assume that the XUV photoelectron and Auger electron spectra do not overlap ($\mathbf{k}_x \neq \mathbf{k}_l$.) The Hamiltonian is (in atomic units $\hbar = m_e = e^2 = 1$)

$$H(t) = \sum_j -\frac{\Delta_j}{2} + U_j + \frac{1}{|\mathbf{r}_2 - \mathbf{r}_3|} - \mathcal{E}_x(t)z_1 - \mathcal{E}_l(t)z_3, \quad (7)$$

with the Laplacians Δ_j acting on the respective electron coordinates $\mathbf{r}_j$, $j = 1, 2, 3$, and effective single-electron potentials $U_j(\mathbf{r}_j)$. The electric fields are assumed to be polarized in z direction. The laser field will be specified later and the XUV field is given as

$$\mathcal{E}_x(t) = \mathcal{E}_0(t)[e^{it\Omega} + e^{-it\Omega}] \quad (8)$$

with pulse envelope $\mathcal{E}_0(t)$. The Hamiltonian (7) neglects the influence of the laser field on the XUV photoelectron and the action of the XUV pulse on the Auger electron. We make the ansatz for the wave function

$$\Psi(t) = c_g(t)|g\rangle + \int dk_x^{(3)}\, c_h(\mathbf{k}_x, t)|h\rangle + \int dk_x^{(3)}\, dk_l^{(3)}\, c_f(\mathbf{k}_x, \mathbf{k}_l, t)|f\rangle, \quad (9)$$

with the initial conditions $c_g(t = -\infty) = 1$ and $c_h(t = -\infty) = c_f(t = -\infty) = 0$.

Using the property of the Volkov states $i\partial_t|\mathbf{k}_\eta, t\rangle = [-\Delta/2 + \mathcal{E}_\eta(t)z]|\mathbf{k}_\eta, t\rangle$ and assuming that $|0\rangle$, $|a\rangle$, and $|b\rangle$ are (approximate) eigenstates of the respective operators $-\Delta_j/2 + U_j$ and that the ground state is depleted little $c_g(t) \approx 1$ one obtains the equations for c_h and c_f

$$i\dot{c}_h(\mathbf{k}_x, t) = D(\mathbf{k}_x, t) + \int dk_1^{(3)} M^*(\mathbf{k}_l, t)c_f(\mathbf{k}_x, \mathbf{k}_1, t), \quad (10)$$

$$i\dot{c}_f(\mathbf{k}_x, \mathbf{k}_l, t) = M(\mathbf{k}_l, t)c_h(\mathbf{k}_x, t). \quad (11)$$

The XUV dipole transition appears in

$$D(\mathbf{k}_x, t) = -\mathcal{E}_0(t)e^{i\Phi_x(\mathbf{k}_x, t) - it(E_0 + \Omega)} d(\mathbf{k}_x - \mathbf{A}_x), \quad (12)$$

where $d(\mathbf{k})$ is the dipole matrix element of XUV-induced transition. The Auger transition matrix element is

$$M(\mathbf{k}_l, t) = \langle 0, t|\langle \mathbf{k}_l, t| \frac{1}{|\mathbf{r}_2 - \mathbf{r}_3|} |b, t\rangle|a, t\rangle. \quad (13)$$

These equations include a few more approximations. It is assumed that all single-electron states are orthogonal to each other. The continuum electrons do not feel the U_j potentials. The latter is a standard approximation in strong field physics and can be safely assumed to be valid for electron energies far from continuum threshold. Near threshold, the most important effect of the atomic potential is an enhancement of the photoionization yield. Similarly, we neglect continuum-continuum transitions between Volkov states. This excludes "post-collision interactions" [6,11] of photoelectron and Auger electron, which is outside the scope of the present work.

Equations (10) and (11) were solved numerically for parameters studied in Ref. [4]: XUV photon energy $\Omega = 90\,\text{eV}$, electron levels $E_0 = -75\,\text{eV}$, $E_a = E_b = -15\,\text{eV}$, and laser photon energy of $\omega = 1.55\,\text{eV}$ ($\lambda = 800$ nm). The $|0\rangle$, $|a\rangle$, and $|b\rangle$ states represent the $3d$, $4s$, and $4p$ orbitals of krypton, respectively. For the questions investigated here, the exact shape of the electron orbitals is of little importance and therefore we chose hydrogenic wave functions with the corresponding principal and orbital quantum numbers. The radial coordinates of the orbitals were scaled to fit the approximate spatial extension of the Kr orbitals and to produce the correct asymptotic behavior for the respective energies. The $4s \rightarrow 3d$ transition singles out the quadrupole term of the electron-electron interaction and justifies the factorization

$$M(\mathbf{k}_l, t) \approx Q_{a0}\, q(\mathbf{k}_l - \mathbf{A}_l(t))e^{-itW_A + i\Phi_l(\mathbf{k}_l, t)}, \quad (14)$$

where $q(\mathbf{k})$ is the quadrupole matrix element for the transition from $|b\rangle$ into the continuum. The strength Q_{a0} of the quadrupole transition $|a\rangle \rightarrow |0\rangle$ was chosen as a parameter to control the Auger decay rate Γ.

Three resulting laser-streaked Auger spectra are shown in Fig. 2 for XUV-pulse duration 500 as FWHM and Auger decay times 200 as, 500 as (1 as $= 10^{-18}$ s), and 2 fs. The observation direction is parallel to laser polarization. A Gaussian laser pulse with duration of 6.5 fs FWHM duration and peak intensity $5 \times 10^{11}\,\text{W/cm}^2$ was assumed. The general characterisitcs of the spectra are determined by the duration of the whole process consisting of XUV excitation and Auger decay compared to the laser optical cycle of $\sim$2.6 fs. For fast Auger decay the main effect of streaking is a shift of the spectrum, which depends on the delay between the laser and the XUV

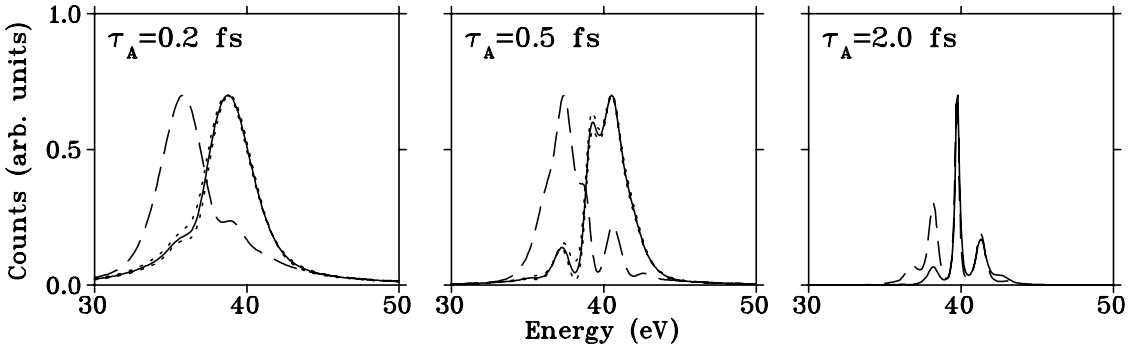

FIG. 2. Streaked Auger electron spectra for different Auger life times τ_A. XUV-laser delay times are $\Delta t = 0$ (solid lines) and π/ω (dashed). Spectra for XUV pulse duration of $\tau_x = 300$ as (lower dotted lines) and 700 as (upper dotted lines) nearly coincide with spectra for 500 as.

pulse. The spectra resemble the streaked photoelectron spectra of [3]. For slow Auger decay, however, pronounced sidebands of the Augerline are formed. This regime corresponds to the first time-domain observation of the Auger decay [4]. The impact of the XUV-pulse duration on the spectra is relatively small as long as the variation of τ_x is small in comparison with the Auger decay time.

A more detailed understanding of the streaked spectra can be obtained from an analytic solution for c_f. We first derive the amplitude in the absence of the laser probe pulse. With the assumption that c_h is a slowly varying function and using the rotating wave approximation for the XUV field one obtains

$$c_h(\mathbf{k}_x, t) = \frac{d(\mathbf{k}_x)}{2\pi} \int_{-\infty}^{\infty} \frac{\tilde{\mathcal{E}}_0(\eta) \exp[i(\mathbf{k}_x^2/2 - W_x - \eta)t]}{\mathbf{k}_x^2/2 - W_x - \Delta - \eta - i\Gamma/2} d\eta, \tag{15}$$

where $\tilde{\mathcal{E}}_0$ is the Fourier transform of the XUV envelope $\mathcal{E}_0$. Auger energy shift Δ and width Γ can be calculated in second order perturbation theory and by Fermi's golden rule, respectively. The final two-electron amplitude without laser field is obtained by substituting (15) into (11)

$$c_f(\mathbf{k}_x, \mathbf{k}_l, \infty) = Q_{a0}\, d(\mathbf{k}_x) q(\mathbf{k}_l) s(\mathbf{k}_x^2, \mathbf{k}_l^2), \tag{16}$$

where we have defined the two-electron line shape

$$s(\mathbf{k}_x^2, \mathbf{k}_l^2) := \frac{\tilde{\mathcal{E}}_0(\mathbf{k}_x^2/2 + \mathbf{k}_l^2/2 - \Omega - E_a - E_b)}{\mathbf{k}_l^2/2 - W_A - \Delta + i\Gamma/2}. \tag{17}$$

In the absence of resonances and far from threshold dipole- and Auger matrix elements d and q are slowly varying functions of $|\mathbf{k}_x|$ and $|\mathbf{k}_l|$, respectively. The shape of the two-electron spectrum is determined by the Lorentzian line shape of the Auger decay and by the spectral envelope of the XUV pulse. The width of the Auger spectrum is proportional to Γ.

A closed form solution for laser-streaked electron spectra is obtained, when one neglects the impact of the laser field on c_h by using expression (15) for c_h also when the laser field is present. From a physics point of view, one does not expect the laser action on the free Auger electrons to affect the core-hole state amplitude c_h. We verified this numerically by suppressing laser action on c_h, which, for our parameter range, changed the spectra on the subpercent level. In this approximation, one can perform all integrations for a cw laser field $\mathbf{A}_l(t) = \mathcal{A}_0 \sin\omega(t + \Delta t)$. Neglecting terms quadratic in $\mathbf{A}_l$ and expanding $\exp[i\mathbf{k}_l \cdot \mathbf{A} \sin\omega t]$ into Bessel functions yields

$$\begin{aligned} c_f(\mathbf{k}_x, \mathbf{k}_l, \infty) = {} & Q_{a0}\, d(\mathbf{k}_x) q(\mathbf{k}_l) \\ & \times \sum_n e^{in(\omega\Delta t + \pi)} J_n\left(\frac{\mathbf{k}_l \cdot \mathcal{A}_0}{\omega}\right) \\ & \times s(\mathbf{k}_x^2, \mathbf{k}_l^2 + 2n\omega). \end{aligned} \tag{18}$$

This formula has a straightforward physical interpretation. The overall electron yield grows linearly with XUV intensity due to the linearity of the XUV single-photon ionization process [c.f. Eq. (17)]. The spectral shape is modified by the laser pulse. Independent of XUV-pulse duration and Auger decay time, there is always a set of sidebands shifted by energies $\pm n\omega$, whose number increases with laser intensity like $n \sim \mathbf{k}_l \cdot \mathcal{A}_0/\omega$. The width of the shape function $s(\mathbf{k}_x^2, \mathbf{k}_l^2)$ determines whether these lines interfere or not. When the lines are narrow, they do not affect each other and one observes the standard sideband structure with peak amplitudes proportional to J_n. When the lines are broad, interference is governed by the delay-dependent phases $\exp(in\omega\Delta t)$, leading to a shift of the center of gravity of the spectrum across the spectral range as the delay Δt varies by one optical period (cf. Fig. 2). The effect is easiest to understand at lower laser intensities, where only $n = -1$, 0, and 1 contribute. If, for example, destructive interference between $n = 0$ and $n = 1$ components occurs at $\Delta t = 0$, it becomes constructive at $\Delta t = \pi/\omega$, shifting the spectrum from the lower to the upper sideband.

Next we investigate the accuracy of the closed form solution. Figure 3 shows spectra obtained from Eqs. (10) and (11) and from (18). For the comparison, a cw laser

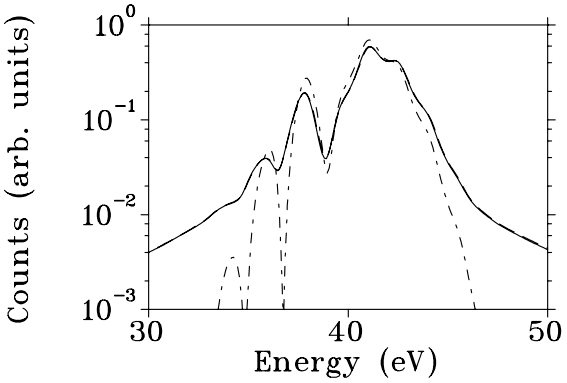

FIG. 3. Auger electron spectrum for a 500 as pulse and 500 as Auger life time. The full model (solid line) coincides with the spectrum using Eq. (18) within the resolution of the plot. The *ad hoc* formula used in Ref. [4] (dot-dashed) produces a narrower spectrum. The curves are normalized to have equal integral.

field was used and it was assumed that the matrix elements d and M are independent of $\mathbf{A}_I$. For the given parameters the results coincide within the resolution of the plot, which confirms the assumptions made for the derivation of Eq. (18). We found the same excellent agreement for the whole range of parameters used here. For general pulse shapes Eq. (18) can be extended by expanding the laser pulse envelope in the form $\mathcal{A}(t) \approx \mathcal{A}_0 + t\dot{\mathcal{A}}_0 + t^2\ddot{\mathcal{A}}_0/2$, where $t = 0$ coincides with the peak of the XUV pulse.

To detect effects of quantum coherence in the pump-probe measurement, we compared our results with the *ad hoc* formula employed in Ref. [4]. That formula essentially amounts to setting the hole state amplitude in Eq. (11) to $c_h(\mathbf{k}_x, t) \approx \sqrt{\rho(t)}$, where ρ is the population of the hole state obtained from the rate equations for XUV ionization and Auger decay. It can be understood as a two-stage description of first core-hole formation and then Auger decay, where the decay is not influenced by the formation. In contrast, in the present quantum model a record about how the hole state was formed is kept in the $\mathbf{k}_x$-dependent phase $\sim\exp(it\mathbf{k}_x^2/2)$ of c_h [cf. Eq. (15)]. As quantum phase coherence between formation and decay is maintained, the *sum* of the electron kinetic energies $\mathbf{k}_x^2/2 + \mathbf{k}_I^2/2$ enters the argument of $\tilde{\mathcal{E}}_0$ in Eq. (17). The final state amplitude c_f cannot be factorized into the product of single-electron amplitudes, indicating the presence of quantum correlations between XUV electrons and Auger electrons. It is important to note that the phase coherence is the only source of correlations of XUV electrons and Auger electrons: no Coulomb interaction, exchange interaction, or rearrangement of the electrons are assumed in the present model. Using Eq. (17) one can see that the degree of correlation is controlled by the parameter $\Gamma\tau_x$, with the correlations increasing for $\Gamma\tau_x > 1$. In the two-step *ad hoc* model, the absence of $\mathbf{k}_x$ dependence in ρ removes all coherence between XUV ionization and Auger decay. The most conspicuous consequence is that the width of Auger spectra is underestimated by the *ad hoc* model. For $\Gamma\tau_x \gg 1$ the discrepancies become severe and preclude a two-stage description of the process.

The presence of strong correlations between photoelectron and Auger electron energies may be exploited for streaking of selected parts of the Auger line in case of very fast Auger decay, when the large width of the spectra does not allow effective streaking of the whole Auger line. When one selects a fixed photoelectron energy $\mathbf{k}_x^2/2$, the energy correlation that appears in the quantum coherent solution restricts the range of possible Auger energies to within the spectral width of the XUV pulse $\sim 1/\tau_x$, which may be much narrower than Γ.

In summary, the theory formulated here establishes a basic framework for the description of time-resolved measurements by the new attosecond pump-probe methods. We have shown how effects of quantum coherence can be treated correctly and we have pointed out their importance for the laser-streaked spectra. The analytic formula for the amplitudes can be employed for a computationally efficient and quantitatively accurate analysis of the spectra. In concentrating on the basic quantum mechanical questions we have deliberately excluded much of the complexity connected with few-electron processes in atomic physics. Most importantly, electron correlation and electron-electron interactions will lead to various types of shake processes and post-collision interaction. Models for these processes used in traditional atomic spectroscopy can be added to our theory.

We thank F. Krausz, M. Ivanov, and J. Burgdörfer for illuminating discussions. This work was supported by the Austrian Science Fund special research programs F011 and F016, and Project No. M718-N08.

*Electronic address: scrinzi@tuwien.ac.at

[1] P. M. Paul *et al.*, Science **292**, 1689 (2001).
[2] M. Hentschel *et al.*, Nature (London) **414**, 509 (2001).
[3] R. Kienberger *et al.*, Science **297**, 1144 (2002).
[4] M. Drescher *et al.*, Nature (London) **419**, 803 (2002).
[5] E. Constant, V. D. Taranukhin, A. Stolow, and P. B. Corkum, Phys. Rev. A **56**, 3870 (1997).
[6] T. Åberg, Phys. Scr. **T41**, 71 (1992).
[7] M. V. Fedorov and A. E. Kazakov, Prog. Quantum Electron. **13**, 1 (1989).
[8] P. Lambropoulos and P. Zoller, Phys. Rev. A **24**, 379 (1981).
[9] J. Itatani *et al.*, Phys. Rev. Lett. **88**, 173903 (2002).
[10] M. Kitzler *et al.*, Phys. Rev. Lett. **88**, 173904 (2002).
[11] H. P. Saha, Phys. Rev. A **42**, 6507 (1990).